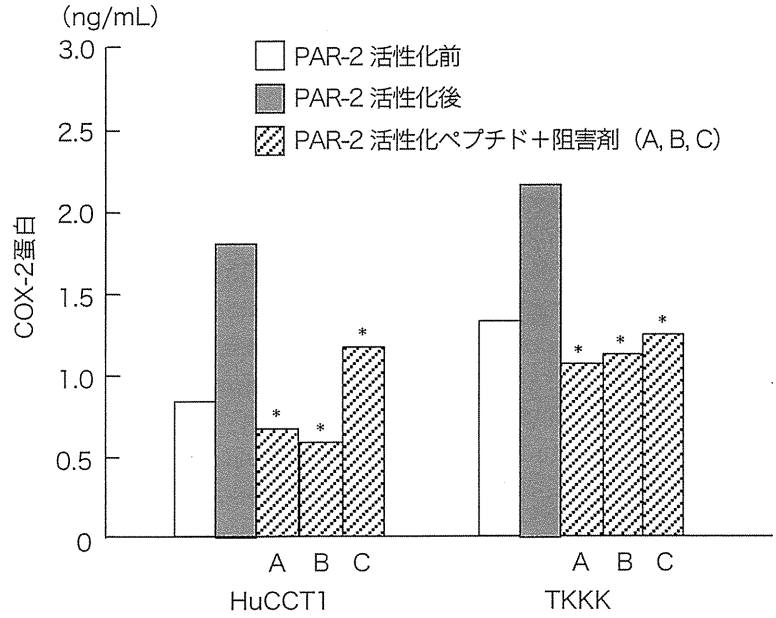

図3　PAR-2発現胆管細胞株(HuCCT1・TKKK)におけるCOX-2蛋白の発現の変化(文献9より引用改変)

活性化ペプチド投与によりCOX-2蛋白の発現は亢進し，MAPK阻害薬(A・B)およびNF-κB阻害薬(C)追加投与によりそれらは減弱化した．*p<0.05. vs. PAR-2活性化後

活性化によるCOX-2の発現亢進が抑制された(図3)[9]．したがって，胆管癌におけるPAR-2・COX-2増殖経路にはMAPKだけでなくNF-κBの関与が示されたこととなった．

4 胆管癌と治療薬としてのNF-κB阻害薬

現在，日常臨床で使用されているNF-κB阻害能をもつ薬剤として，多発性骨髄腫に適応があるプロテアソーム阻害薬，ボルテゾミブなどがある[21]．しかし，NF-κBは免疫や造血を含めた多くの生理現象に関わっており，さらにアポトーシスの誘導にも関わることも示されている．したがって腫瘍に対するNF-κB阻害薬の開発には種々の生理現象への影響を小さくしつつ抗癌作用を保つことが重要となる[22]．胆管癌においても，近年，その増殖・進展・浸潤へのNF-κBの関与を示唆する報告が散見される．Seubwaiらは，抗炎症・抗アレルギー作用をもつcepharanthineは，NF-κBを阻害することにより胆管癌の抗腫瘍活性を示すと報告した[23]．Prakobwongらは，ポリフェノールの一種である，抗酸化作用・抗炎症作用をもつcurcuminがDNA結合・核内移行・p65リン酸化などの過程でNF-κB活性化を阻害するとしている[24]．またDaiらは，NF-κB経路を介した胆管癌の増殖進展において胆汁酸が調節に関与することを示した[25]．遊離胆汁酸は細胞死を促進することにより胆管癌の進展を阻害し，一方で抱合胆汁酸は腫瘍増殖を促進すると報告している．ただし，いずれの論文もPAR-2・COX-2経路によるものでなくわれわれの報告とは異なるものである．また現時点ではいずれの報告も*in vitro*や*in vivo*での実験レベルのものにとどまり，臨床応用の報告はなされていない．胆管癌は手術が唯一の根治治療であり，切除不能・再発例に対して

化学療法が選択されるが抵抗性を示すことも多い．その理由としてさまざまな腫瘍増殖因子がその増殖・浸潤に関わることがあげられている[26-29]．NF-κBだけでなく複数の増殖経路に依存する胆管癌においては，複数の阻害薬の組み合わせにより治療戦略を立てるのが重要と考えられる[21]．さらなる胆管癌に対する新規治療薬の開発が期待される．

5 おわりに

胆管癌におけるPAR-2・COX-2経路ならびにNF-κB活性と腫瘍増殖の関連性について述べた．胆管癌に対する化学療法の治療薬としての，NF-κB阻害薬を含めた臨床的薬剤のさらなる開発が必要と考えられている．

文　献

1) 厚生労働省大臣官房統計情報部：人口動態統計．厚生労働省ホームページ．http://www.mhlw.go.jp/toukei/saikin/index.html
2) 正田純一：胆道癌，肝内胆管癌のリスクファクターとその発癌・進展のメカニズム．胆と膵 34：455–460, 2013
3) Baldwin AS Jr：The NF-kappa B and I kappa B proteins: new discoveries and insights. Annu Rev Immunol 14：649–683, 1996
4) Ghosh S, May MJ, Kopp EB：NF-kappa B and Rel proteins: evolutionarily conserved mediators of immune responses. Annu Rev Immunol 16：225–260, 1998
5) Barkett M, Gilmore TD：Control of apoptosis by Rel/NF-kappaB transcription factors. Oncogene 18：6910–6924, 1999
6) Shibata K, Yada K, Matsumoto T et al：Protease-activating-receptor-2 is frequently expressed in papillary adenocarcinoma of the gallbladder. Oncol Rep 12：1013–1016, 2004
7) Yada K, Shibata K, Matsumoto T et al：Protease-activated receptor-2 regulates cell proliferation and enhances cyclooxygenase-2 mRNA expression in human pancreatic cancer cells. J Surg Oncol 89：79–85, 2005
8) Iwaki K, Shibata K, Ohta M et al：A small interfering RNA targeting proteinase-activated receptor-2 is effective in suppression of tumor growth in a Panc1 xenograft model. Int J Cancer 122：658–663, 2008
9) Eguchi H, Iwaki K, Shibata K et al：Protease-activated receptor-2 regulates cyclooxygenase-2 expression in human bile duct cancer via the pathways of mitogen-activated protein kinase and nuclear factor kappa B. J Hepatobiliary Pancreat Sci 18：147–153, 2011
10) Nystedt S, Emilsson K, Wahlestedt C et al：Molecular cloning of a potential proteinase activated receptor. Proc Natl Acad Sci U S A 91：9208–9212, 1994
11) Houliston RA, Keogh RJ, Sugden D et al：Protease-activated receptors upregulate cyclooxygenase-2 expression in human endothelial cells. Thromb Haemost 88：321–328, 2002
12) Frungieri MB, Weidinger S, Meineke V et al：Proliferative action of mast-cell tryptase if mediated by PAR2, COX2, prostaglandins, and PPARgamma: Possible relevance to human fibrotic disorders. Proc Natl Acad Sci U S A 99：15072–15077, 2002
13) Eberhart CE, Coffey RJ, Radhika A et al：Up-regulation of cyclooxygenase 2 gene expression in human colorectal adenomas and adenocarcinomas. Gastroenterology 107：1183–1188, 1994
14) Ristimäki A, Honkanen N, Jänkälä H et al：Expression of cyclooxygenase-2 in human gastric carcinoma. Cancer Res 57：1276–1280, 1997
15) Zimmermann KC, Sarbia M, Weber AA et al：Cyclooxygenase-2 expression in human esophageal carcinoma. Cancer Res 59：198–204, 1999
16) Wolff H, Saukkonen K, Anttila S et al：Expression of cyclooxygenase-2 in human lung carcinoma. Cancer Res 58：4997–5001, 1998
17) Syeda F, Grosjean J, Houliston RA et al：Cyclooxygenase-2 induction and prostacyclin release by protease-activated receptors in endothelial cells require cooperation between mitogen-activated protein kinase and NF-kappaB pathways. J Biol Chem 281：11792–11804, 2006
18) Wang H, Wen S, Bunnett NW et al：Proteinase-activated receptor-2 induces cyclooxygenase-2 expression through beta-catenin and cyclic AMP-response element-binding protein. J Biol Chem 283：809–815, 2008
19) Jikuhara A, Yoshii M, Iwagaki H et al：MAP kinase-mediated proliferation of DLD-1 carcinoma by the stimulation of protease-activated receptor 2. Life Sci 73：2817–2829, 2003

20) Yoon JH, Higuchi H, Werneburg NW et al : Bile acids induce cyclooxygenase-2 expression via the epidermal growth factor receptor in a human cholangiocarcinoma cell line. Gastroenterology 122 : 985–993, 2002
21) 得平道英，木崎昌弘：NF-κB阻害剤．医学のあゆみ242 : 1194–1201, 2012
22) 堀江良一：NF-κB阻害薬のがん治療への臨床応用．実験医学（増刊）30, No.5 : 212–218, 2012
23) Seubwai W, Vaeteewoottacharn K, Hiyoshi M et al : Cepharanthine exerts antitumor activity on cholangiocarcinoma by inhibiting NF-kappaB. Cancer Sci 101 : 1590–1595, 2010
24) Prakobwong S, Gupta SC, Kim JH et al : Curcumin suppresses proliferation and induces apoptosis in human biliary cancer cells through modulation of multiple cell signaling pathways. Carcinogenesis 32 : 1372–1380, 2011
25) Dai J, Wang H, Dong Y et al : Bile acids affect the growth of human cholangiocarcinoma via NF-kappaB pathway. Cancer Invest 31 : 111–120, 2013
26) Sirica AE : Cholangiocarcinoma: molecular targeting strategies for chemoprevention and therapy. Hepatology 41 : 5–15, 2005
27) Hassid V, Orlando FA, Awad ZT et al : Genetic and molecular abnormalities in cholangiocarcinogenesis. Anticancer Res 29 : 1151–1156, 2009
28) Fava G, Marzioni M, Benedetti A et al : Molecular pathology of biliary tract cancers. Cancer Lett 250 : 155–167, 2007
29) 中沼安二，佐藤保則，佐々木素子，他：慢性胆管上皮障害からみた肝内胆管癌のハイリスク因子．肝胆膵57 : 27–33, 2008

*　　*　　*

J Hepatobiliary Pancreat Sci (2014) 21:288–295
DOI: 10.1002/jhbp.26

ORIGINAL ARTICLE

Mammalian target of rapamycin signaling activation patterns in pancreatic neuroendocrine tumors

Yoko Komori · Kazuhiro Yada · Masayuki Ohta · Hiroki Uchida · Yukio Iwashita · Kengo Fukuzawa · Kenji Kashima · Shigeo Yokoyama · Masafumi Inomata · Seigo Kitano

Published online: 3 September 2013

Abstract
Background Phosphatidylinositol 3-kinase/Akt/mammalian target of rapamycin (mTOR) pathway dysregulation has been implicated in the development of various human cancers. However, expression of mTOR cascade components in pancreatic neuroendocrine tumors (PNETs) has not been fully explored. The aim of this study was to assess the expression of mTOR pathway in PNETs using immunohistochemistry.
Methods From December 1984 to April 2012, we surgically treated 42 patients with PNETs. We used immunohistochemistry to evaluate expression of mTOR, phosphorylated mTOR (p-mTOR), p70S6 kinase (S6K), phosphorylated S6 ribosomal protein (p-S6rp), eukaryotic initiation factor 4E-binding protein 1 (4E-BP1), and phosphorylated 4E-BP1 (p-4E-BP1) in the resected specimens. The relation between the expression of these molecules and clinicopathological characteristics was investigated.
Results We identified the expression of mTOR (28.6%), p-mTOR (52.4%), S6K (52.4%), p-S6rp (40.5%), 4E-BP1 (81.0%), and p-4E-BP1 (26.2%) in PNETs. The expression of mTOR, p-mTOR, S6K, and p-S6rp was significantly associated with tumor invasion, proliferation, and an advanced-stage. Particularly, the expression of p-mTOR was related to clinically relevant factors such as tumor size, vascular invasion, extrapancreatic invasion, lymph node and/or distant metastasis, mitotic count, and European Neuroendocrine Tumor Society TNM staging as well as the 2004 and 2010 World Health Organization (WHO) classification. In addition, p-S6rp expression was related to vascular invasion, extrapancreatic invasion, lymph node and distant metastasis, mitotic count, and the 2010 WHO classification. In contrast, no significant relation between 4E-BP1 activation and clinicopathological factors was observed. The expression of p-mTOR was strongly correlated with that of p-S6rp ($r = 0.474$, $P = 0.002$).
Conclusions Our results suggest that activation of the mTOR/S6K signaling pathway plays a significant role in tumorigenesis and progression of PNET.

Keywords Immunohistochemistry · Mammalian target of rapamycin inhibitor · Mammalian target of rapamycin signaling pathway · Pancreatic neuroendocrine tumors

Y. Komori (✉) · K. Yada · M. Ohta · H. Uchida · Y. Iwashita · M. Inomata
Department of Gastroenterological and Pediatric Surgery, Oita University Faculty of Medicine, 1-1 Idaigaoka, Hasama-machi, Yufu, Oita 879-5593, Japan
e-mail: komorin@oita-u.ac.jp

K. Fukuzawa
Department of Surgery, Oita Red Cross Hospital, Oita, Japan

K. Kashima · S. Yokoyama
Department of Diagnostic Pathology, Oita University Faculty of Medicine, Oita, Japan

S. Kitano
Oita University, Oita, Japan

Introduction

Pancreatic neuroendocrine tumors (PNETs) are believed to be rare and are derived from mature endocrine cells or multipotent stem cells with neuroendocrine characteristics [1, 2]. The incidence rate of PNETs in the United States between 2002 and 2004 was estimated as 0.32 per 100 000 people, per year [3]. In Japan, the incidence rate of PNETs in 2005 was estimated as 1.01 per 100 000 people [4], approximately three times the incidence in the United

States. Furthermore, PNETs incidence in Japan has increased over the last two decades [5].

Pancreatic neuroendocrine tumors can produce insulin, gastrin, glucagon, vasoactive intestinal peptide (VIP), and somatostatin, although hormone-producing PNETs do not always cause symptoms related to hormone overproduction. Because PNETs are considered to be potentially malignant tumors, radical surgery is the only curative treatment. Drug treatment with somatostatin analogs and molecular target therapy has been performed for patients who do not benefit from surgery alone [4].

Mammalian target of rapamycin (mTOR) is a highly conserved serine/threonine kinase located downstream of the phosphatidylinositol 3-kinase (PI3K)/Akt signaling pathway, which regulates several cellular functions such as protein synthesis, cell proliferation, cell metabolism and angiogenesis [6, 7]. mTOR signaling is positively regulated by hormones, growth factors and amino acids [8, 9]; phosphorylated mTOR (p-mTOR) sequentially activates downstream targets including p70S6 kinase (S6K) and eukaryotic initiation factor 4E-binding protein 1 (4E-BP1) [10]. S6K subsequently phosphorylates the S6 ribosomal protein (S6rp) of the 40S ribosomal subunit, which initiate protein synthesis. Phosphorylation of 4E-BP1 by mTOR releases eukaryotic initiation factor 4E (eIF4E) from 4E-BP1, which initiates mRNA translation of several genes necessary for cell cycle progression [10].

Mammalian target of rapamycin is a critical effector in cell-signaling pathways for several human cancers, including ovarian cancer [11, 12], breast cancer [13], urothelial carcinoma [14], biliary tract adenocarcinoma [15], and hepatocellular carcinoma [16–18]. In each of these cancers, mTOR upregulation and/or activation has been observed. In addition, upregulation of this pathway is related to a poor prognosis of ovarian cancer, urothelial carcinoma, and biliary tract adenocarcinoma.

Several mTOR inhibitors have been available for treatment to date, including everolimus (RAD001, Afinitor, Novartis Pharmaceuticals, Basel, Switzerland) and its analogs, temsirolimus (CCI-779, Torisel, Wyeth Pharmaceuticals, Philadelphia, PA, USA) and ridaforolimus (AP23573, formerly Deforolimus, Ariad Pharmaceuticals, Cambridge, MA, USA) [19–21]. Recently, RADIANT-03 phase III trial demonstrated that everolimus, compared with placebo, improved progression-free survival in patients with advanced PNETs [22]. In addition, a recent study reported that the expression of mTOR and activation of PNETs were evaluated using immunohistochemistry, and extensive expression of mTOR and p-mTOR was identified [23]. However, data on the activation status of the mTOR signaling cascade in PNETs is still lacking. Therefore, the purpose of the present study was to evaluate the expression of activated mTOR and its downstream targets, S6K and 4E-BP1, in PNETs and to investigate the relation between the expression and clinicopathological data.

Materials and methods

Patients

Between December 1984 and April 2012, 42 patients (28 women, 14 men; mean age, 60 years; range, 19–84 years) with primary PNETs underwent surgery at the Department of Gastroenterological and Pediatric Surgery, Oita University Faculty of Medicine, or the related hospitals including Oita Red Cross Hospital, Oita Medical Center (Oita, Japan), and Beppu Medical Center (Beppu, Japan). The status of the PNETs (size, number, location, and gloss classification) was evaluated on the basis of routine imaging modalities, including enhanced computed tomography and magnetic resonance imaging. All specimens were diagnosed using immunohistochemistry in the routine diagnostic setting. By convention, antibodies against chromogranin A and synaptophysin were used to ensure neuroendocrine differentiation. On the basis of the 2004 and 2010 World Health Organization (WHO) classification, these tumors were classified into well-differentiated neuroendocrine tumors (WDNET), well-differentiated neuroendocrine carcinomas (WDNEC), poorly-differentiated neuroendocrine carcinomas (PDNEC), neuroendocrine tumor (NET) G1, NET G2, and neuroendocrine carcinomas (NEC) [24]. The clinical staging was based on the TNM classification by the European Neuroendocrine Tumor Society (ENETS) [25]. Information on clinical follow-up and survival was obtained for all patients. This research protocol was approved by the Ethics Committee of the Oita University Faculty of Medicine.

Immunohistochemistry

All tissue specimens were immunostained using the biotin-streptavidin method and a Histofine kit (Nichirei, Tokyo, Japan). The antibodies used by us for immunostaining are summarized in Table 1. All antibodies were purchased from Cell Signaling Technologies (Danvers, MA, USA). Sections (3-μm thick) were cut from formalin-fixed paraffin-embedded tissues and placed on silanized slides. The tissue sections were deparaffinized in xylene and rehydrated using a graded series of ethanols. Endogenous peroxidase activity was blocked for 20 min with 3% hydrogen peroxidase. Antigen retrieval was performed by placing the slides in 10 mM citrate buffer (pH 6.0) and heating them in an autoclave at 121°C for 15 min. These slides were further incubated with primary antibodies overnight in a moist chamber at 4°C. The antigen–antibody complex was subsequently visualized with 3,3′-diaminobenzidine solution for 5 min.

Table 1 Antibodies and their conditions of immunostaining

Primary antibody	Clone	Specificity	Dilution	Source
mTOR	Rabbit mAb, 7C10	/	1/50	
p-mTOR	Rabbit mAb, 49F9	Ser 2448	1/100	
S6K	Rabbit mAb, 49D7	/	1/60	Cell signaling technology
p-S6rp	Rabbit mAb, D57.2.2E	Ser 235/236	1/100	(Danvers, MA, USA)
4E-BP1	Rabbit mAb, 53H11	/	1/800	
p-4E-BP1	Rabbit mAb, 236B4	Thr 37/46	1/50	
Ki-67	Mouse mAb	/	1/50	Dako
				(Glostrup, Denmark)

mAb monoclonal antibody, *Ser* serine, *Thr* threonine

The slides were rinsed again, counterstained with hematoxylin, dehydrated, and cover slipped. Sections of prostate adenocarcinoma were used as a positive control. Negative controls were incubated with the primary antibodies combined with excess blocking peptides of each antibody (mTOR blocking peptide #1072, p-mTOR blocking peptide Ser 2448 #1230, S6K blocking peptide #1205, Phospho-S6 Ribosomal Protein blocking peptide Ser235/236 #1220, 4E-BP1 blocking peptide #1053, Phospho-4E-BP1 blocking peptide Thr37/46 #1052, Cell Signaling Technology). The ratio of blocking peptide to antibody was 5:1.

Evaluation of immunohistochemistry

Immunoreactivity for mTOR, p-mTOR, S6K, p-S6rp, 4E-BP1, and p-4E-BP1 was recognized in the cytoplasm of tumor cells. Staining of mTOR, p-mTOR, S6K, p-S6rp, 4E-BP1, and p-4E-BP1 in the tumor tissue was scored by applying a semi-quantitative immunoreactivity scoring (IRS) system, as previously described [26, 27]. In brief, category A indicated the staining intensity as 0 (negative), 1 (weak), 2 (moderate), or 3 (strong). Category B indicated the percentage of immunoreactive cells as 0 (none), 1 (<10%), 2 (10%–50%), 3 (51%–80%), 4 (>80%). Multiplication of categories A and B resulted in an IRS ranging from 0 to 12 for each case. An IRS between 1 and 12 was considered positive, and an IRS 0 was considered negative in the relation analysis between the expression and clinicopathological variables. In addition, the raw expression scores were used in the correlation analysis. Immunoreactivity for Ki-67 in the nucleus of tumor cells was evaluated for >1000 cells, and the percentage of immunoreactivity (i.e., labeling index [LI]) was calculated. A specialized pathologist, who was unaware of the patients' clinical characteristics evaluated immunoreactivity for all specimens using light microscopy.

Statistical analysis

Statistical analysis was carried out using Dr. SPSS II software for Windows (version 11.01 J; SPSS Japan, Tokyo, Japan). The significance of the relationship between the expression of mTOR, p-mTOR, S6K, p-S6rp, 4E-BP1, and p-4E-BP1 and clinicopathological characteristics was tested using Fisher's exact test and a χ^2 test. The correlation among mTOR, p-mTOR, S6K, p-S6rp, 4E-BP1, and p-4E-BP1 expression scores was analyzed using Spearman's rank order correlation. A univariate analysis of disease-free survival was performed using a log-rank test. Factors with P-values of <0.1 in the univariate analysis were used in a subsequent multivariate analysis with a proportional hazards model. P-values < 0.05 were considered statistically significant.

Results

Patient characteristics

The clinicopathological characteristics of 42 patients (28 women, 14 men) are summarized in Table 2. Based on our data and previous data reported in Japan, age was classified into two categories as either ≦60 or >60 years of age [5]. Within this patient group, there were 14 functional and 28 non-functional PNET patients. Of these 42 patients, 12 (28.6%) had vascular invasion, 11 (26.2%) had extrapancreatic invasion, and 8 (19.0%) had lymph node and/or distant metastasis.

Expression of mTOR, p-mTOR, S6K, p-S6rp, 4E-BP1 and p-4E-BP1

Representative immunohistochemical stainings of mTOR, p-mTOR, S6K, p-S6rp, 4E-BP1 and p-4E-BP1 are shown in Figure 1. Immunoreactivity identified expression in the

Table 2 Summary of clinicopathological characteristics

Number of patients	42
Age (years, mean ± SD)	60 ± 15
Sex (female/male)	28/14
Tumor size (mm, mean ± SD)	22.7 ± 21.5
Functionality (functional[a]/non-functional)	14/28
Vascular invasion (No/Yes)	30/12
Extrapancreatic invasion (No/Yes)	31/11
Lymph node and/or distant metastasis (No/Yes)	34/8
Ki-67 labeling index[b] (≦2%/3%–20%)	35/7
Mitotic count[c] (≦2/>2)	36/6
2004 WHO classification (WDNET/WDNEC/PDNEC)	26/14/2
2010 WHO classification (NET G1/NET G2/NEC)	33/8/1
ENETS TNM staging (I/II/III · IV)	25/9/8
Recurrence (No/Yes)	35/7
Prognosis (survival/death)	41/1

[a] All insulinoma

[b] Count multiple regions with highest labeling density, report mean percentage; eyeballed estimate is adequate

[c] Number of mitoses per 10 high-power field or 2 mm^2; count up to 50 high-power fields

ENETS European Neuroendocrine Tumor Society, *NEC* neuroendocrine carcinoma, *NET* neuroendocrine tumor, *PDNEC* poorly-differentiated neuroendocrine carcinomas, *WDNEC* well-differentiated neuroendocrine carcinomas, *WDNET* well-differentiated neuroendocrine tumors, *WHO* World Health Organization

following number of cases: mTOR ($n = 12$; 28.6%), p-mTOR ($n = 22$; 52.4%), S6K ($n = 22$; 52.4%), p-S6rp ($n = 17$; 40.5%), 4E-BP1 ($n = 34$; 81.0%), and p-4E-BP1 ($n = 11$; 26.2%).

Relation between expression of mTOR, p-mTOR, S6K, p-S6rp, 4E-BP1 and p-4E-BP1 and clinicopathological characteristics

The relation between the expression of mTOR signalings and clinicopathological characteristics is shown in Tables 3 and 4. The expression of mTOR was significantly related to mitotic count ($P = 0.046$) and extrapancreatic invasion ($P = 0.006$). The expression of p-mTOR was significantly related to tumor size ($P = 0.023$), 2004 WHO classification ($P = 0.004$), 2010 WHO classification ($P = 0.046$), ENETS TNM staging ($P = 0.007$), mitotic count ($P = 0.022$), functionality ($P = 0.008$), vascular invasion ($P = 0.002$), extrapancreatic invasion ($P = 0.004$), and lymph node and/or distant metastasis ($P = 0.004$). The expression of S6K was significantly related to tumor size ($P = 0.023$), 2010 WHO classification ($P = 0.046$), ENETS TNM staging ($P = 0.025$), and lymph node and/or distant metastasis ($P = 0.047$). The expression of p-S6rp was significantly related to 2010 WHO classification ($P = 0.033$), mitotic count ($P = 0.032$), vascular invasion ($P = 0.006$), extrapancreatic invasion ($P = 0.029$), and lymph node and/or distant metastasis ($P = 0.045$). The expression of 4E-BP1 and p-4E-BP1 were unrelated to any clinicopathological characteristics.

Correlation between the expression of p-mTOR and that of mTOR, S6K, p-S6rp, 4E-BP1 and p-4E-BP1

In the present study, the expression of p-mTOR was associated with several critical clinicopathological data. Therefore, we analyzed the correlation between the expression of

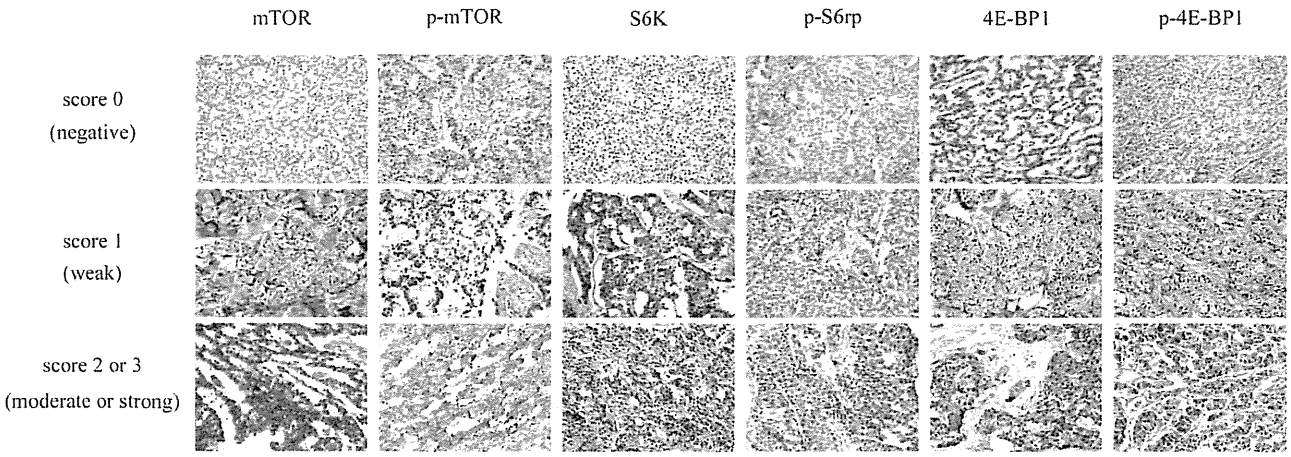

Fig. 1 Representatives immunohistochemical stainings for the expression of mammalian target of rapamycin (mTOR), phosphorylated mTOR (p-mTOR), p70S6 kinase (S6K), phosphorylated S6 ribosomal protein (p-S6rp), 4E-binding protein 1 (4E-BP1), and phosphorylated 4E-BP1 (p-4E-BP1) in pancreatic neuroendocrine tumors (PNETs) (original magnification, 200×). First row, negative (0); second row, weak (1); third row, moderate (2) or strong (3)

Table 3 Relation between the expression of mammalian target of rapamycin (mTOR), phosphorylated mTOR (p-mTOR), p70S6 kinase (S6K), phosphorylated S6 ribosomal protein (p-S6rp), 4E-binding protein 1 (4E-BP1), and phosphorylated 4E-BP1 (p-4E-BP1) and clinical characteristics

Characteristics	*n*	mTOR		p-mTOR		S6K		p-S6rp		4E-BP1		p-4E-BP1	
		Positive	*P*	Positive	*P*	Positive	*P*	Positive	*P*	Positive	*P*	Positive	*P*
Age (years)													
≦60	18	5 (27.8%)	1.0	10 (55.6%)	0.764	10 (55.6%)	0.764	9 (50.0%)	0.348	14 (77.8%)	0.706	5 (27.8%)	1.0
>60	24	7 (29.2%)		12 (50.0%)		12 (50.0%)		8 (33.3%)		20 (83.3%)		6 (25.0%)	
Sex													
Female	28	19 (35.7%)	0.277	12 (42.9%)	0.108	15 (53.6%)	1.0	11 (39.3%)	1.0	22 (78.6%)	0.697	7 (25.0%)	1.0
Male	14	2 (14.3%)		10 (71.4%)		7 (50.0%)		6 (42.9%)		12 (85.7%)		4 (28.6%)	
Tumor size (cm)													
≦2	28	8 (28.6%)	1.0	11 (39.3%)	**0.023**	11 (39.3%)	**0.023**	10 (35.7%)	0.508	21 (75.0%)	0.223	9 (32.1%)	0.283
>2	14	4 (28.6%)		11 (78.6%)		11 (78.6%)		7 (50.0%)		13 (92.9%)		2 (14.3%)	
2004 WHO classification													
WDNET	27	8 (29.6%)	0.72	9 (33.3%)	**0.004**	13 (48.1%)	0.364	8 (29.6%)	0.073	22 (81.5%)	0.736	8 (29.6%)	0.625
WDNEC	13	3 (23.1%)		11 (84.6%)		7 (53.8%)		7 (53.8%)		10 (76.9%)		3 (23.1%)	
PDNEC	2	1 (50.0%)		2 (100%)		2 (100%)		2 (100%)		2 (100%)		0 (0.0%)	
2010 WHO classification													
NET G1	33	7 (21.2%)	0.055	14 (42.4%)	**0.046**	14 (42.4%)	**0.046**	10 (30.3%)	**0.033**	25 (75.8%)	0.26	9 (27.3%)	0.827
NET G2	8	5 (62.5%)		7 (87.5%)		7 (87.5%)		6 (75.0%)		8 (100%)		2 (25.0%)	
NEC	1	0 (0.0%)		1 (100%)		1 (100%)		1 (100%)		1 (100%)		0 (0.0%)	
ENETS TNM													
Stage I	25	6 (24.0%)	0.716	9 (36.0%)	**0.007**	9 (36.0%)	**0.025**	7 (28.0%)	0.06	19 (76.0%)	0.61	7 (28.0%)	0.59
Stage II	9	3 (33.3%)		5 (55.6%)		6 (66.7%)		4 (44.4%)		8 (88.9%)		3 (33.3%)	
Stage III/IV	8	3 (37.5%)		8 (100%)		7 (87.5%)		6 (75.0%)		7 (87.5%)		1 (12.5%)	
Recurrence													
No	35	9 (25.7%)	0.387	17 (48.6%)	0.414	18 (51.4%)	1.0	12 (34.3%)	0.099	27 (77.1%)	0.312	7 (20.0%)	0.063
Yes	7	3 (42.9%)		5 (71.4%)		4 (57.1%)		5 (71.4%)		7 (100%)		4 (57.1%)	
Prognosis													
Survival	41	12 (29.3%)	1.0	21 (51.2%)	1.0	21 (52.1%)	1.0	16 (39.0%)	0.405	33 (80.5%)	1.0	11 (26.8%)	1.0
Death	1	0 (0.0%)		1 (100%)		1 (100%)		1 (100%)		1 (100%)		0 (0.0%)	

F functional, *NEC* neuroendocrine carcinoma, *NET* neuroendocrine tumor, *NF* non-functional, *PDNEC* poorly-differentiated neuroendocrine carcinomas, *WDNEC* well-differentiated neuroendocrine carcinomas, *WDNET* well-differentiated neuroendocrine tumors, *WHO* World Health Organization

Bold denotes statistically significant values

Table 4 Relation between the expression of mammalian target of rapamycin (mTOR), phosphorylated mTOR (p-mTOR), p70S6 kinase (S6K), phosphorylated S6 ribosomal protein (p-S6rp), 4E-binding protein 1 (4E-BP1), and phosphorylated 4E-BP1 (p-4E-BP1) and pathological characteristics

Characteristics	*n*	mTOR		p-mTOR		S6K		p-S6rp		4E-BP1		p-4E-BP1	
		Positive	*P*	Positive	*P*	Positive	*P*	Positive	*P*	Positive	*P*	Positive	*P*
Ki-67 LI													
≦2%	35	8 (22.9%)	0.088	16 (45.7%)	0.096	16 (45.7%)	0.096	12 (34.3%)	0.099	27 (77.1%)	0.312	10 (28.6%)	0.654
3%–20%	7	4 (57.1%)		6 (85.7%)		6 (85.7%)		5 (71.4%)		7 (100%)		1 (14.3%)	
Mitotic count													
<2	36	8 (22.2%)	**0.046**	16 (44.4%)	**0.022**	17 (47.2%)	0.187	12 (34.3%)	**0.032**	28 (77.8%)	0.576	9 (25.0%)	0.644
≧2	6	4 (66.7%)		6 (100%)		5 (83.3%)		5 (83.3%)		6 (100%)		2 (33.3%)	
Functionality													
F	14	5 (28.6%)	0.635	3 (21.4%)	**0.008**	7 (50.0%)	1.0	4 (28.6%)	0.331	9 (64.3%)	0.092	5 (35.7%)	0.459
NF	28	7 (28.6%)		19 (67.9%)		15 (53.6%)		13 (46.4%)		25 (89.3%)		6 (21.4%)	
Vascular invasion													
No	30	7 (23.3%)	0.274	11 (36.7%)	**0.002**	13 (43.3%)	0.091	8 (26.7%)	**0.006**	23 (76.7%)	0.402	8 (26.7%)	1.0
Yes	12	5 (41.7%)		11 (91.7%)		9 (75.0%)		9 (75.0%)		11 (91.7%)		3 (25.0%)	
Extrapancreatic invasion													
No	29	5 (16.1%)	**0.006**	12 (38.7%)	**0.004**	14 (45.2%)	0.166	9 (29.0%)	**0.029**	24 (77.4%)	0.657	9 (29.0%)	0.696
Yes	13	7 (63.6%)		10 (90.9%)		8 (72.7%)		8 (72.7%)		10 (90.9%)		2 (18.2%)	
LN and/or distant metastasis													
No	34	8 (23.5%)	0.195	14 (41.2%)	**0.004**	15 (44.1%)	**0.047**	11 (32.4%)	**0.045**	27 (79.4%)	1.0	10 (29.4%)	0.657
Yes	8	4 (50.0%)		8 (100%)		7 (87.5%)		6 (75.0%)		7 (87.5%)		1 (12.5%)	

F functional, *LI* labeling index, *LN* lymph node, *NF* non-functional

Bold denotes statistically significant values

Table 5 Correlations between the expression of phosphorylated mammalian target of rapamycin (p-mTOR) and that of mTOR, p70S6 kinase (S6K), phosphorylated S6 ribosomal protein (p-S6rp), 4E-binding protein 1 (4E-BP1), and phosphorylated 4E-BP1 (p-4E-BP1)

	mTOR	S6K	p-S6rp	4E-BP1	p-4E-BP1
p-mTOR	$r = 0.193$	$r = 0.230$	$\mathbf{r = 0.474}$	$r = 0.142$	$r = -0.037$
	$P = 0.221$	$P = 0.143$	$\mathbf{P = 0.002}$	$P = 0.370$	$P = 0.817$

Bold denotes statistically significant values

p-mTOR and that of other factors (Table 5). A significant positive correlation was observed between the expression of p-mTOR and p-S6rp ($r = 0.474$, $P = 0.002$). However, the expression of p-mTOR was not significantly correlated with that of mTOR, S6K, 4E-BP1, or p-4E-BP1.

Prognosis and disease-free survival

One patient in the present study died as a result of PNETs. The patient was a 49-year-old woman who underwent a pylorus-preserving pancreaticoduodenectomy for a pancreas head tumor. The tumor was 30 mm in diameter and was diagnosed as WDNEC according to the 2004 WHO classification and NET G1 according to the 2010 WHO classification. The expression of mTOR was negative and that of p-mTOR, S6K, and p-S6rp was positive. The patient died of tumor recurrence with multiple liver, lung and bone metastases 4 years after surgery. Seven patients in the present study had tumor recurrence. In the univariate analysis, ENETS TNM classification ($P = 0.0058$), Ki-67 labeling index ($P = 0.0239$), and lymph node and/or distant metastasis ($P = 0.0019$) were significantly related to the disease-free survival. Expression of mTOR, p-mTOR, S6K, and p-S6rp was not significantly related but showed a tendency toward a relationship ($P < 0.1$). The multivariate analysis revealed that lymph node and/or distant metastasis was an independent factor of disease-free survival ($P = 0.020$).

Discussion

In this study, we evaluated the sequential expression of mTOR, p-mTOR, S6K, p-S6rp, 4E-BP1, and p-4E-BP1, in 42 patients with PNETs. Compared with previous studies, our study has included the largest number of patients in the investigation of the mTOR signaling pathway of PNETs known to date. Our immunohistochemistry analysis of PNETs identified the expression of mTOR (28.6%), p-mTOR (52.4%), S6K (52.4%), p-S6rp (40.5%), 4E-BP1 (81.0%), and p-4E-BP1 (26.2%). The expression rate of p-mTOR was higher than that of mTOR. Although the

reason for this is currently unknown, a similar finding in hepatocellular carcinoma was reported by Sahin et al. [16]. In that study, the expression rate of p-mTOR (15%) was higher than that of total mTOR (5%). The authors suggested that the total mTOR in isolation can miss cases where the pathway was activated. Currently, two studies have demonstrated mTOR signaling pathway activation in PNETs [23, 27]. Kasajima et al. investigated the expression of mTOR and its downstream factors in 99 gastrointestinal and PNET patients using immunohistochemistry and described the expression rates for mTOR (61%), p-S6K (57%), 4E-BP1 (93%), and p-4EBP1 (80%) [27]. Furthermore, strong expression of p-S6K was associated with poor disease-specific survival [27]. In the other study, Zhou et al. reported that the expression rates of mTOR and p-mTOR were 70.6% and 61.8%, respectively [23]. In that study, patients were classified into two groups based on the 2010 WHO classification criteria, and it was concluded that NET G2 patients showed higher mTOR activation rates. The findings from these two studies suggest that the expression and activation of the mTOR pathway has clinical significance in patients with PNETs.

Several recent drug therapies targeting epidermal growth factor receptor (EGFR), vascular endothelial growth factor (VEGF), and human EGFR type 2 (HER2), such as cetuximab, lapatinib, erlotinib, and bevacizumab, also have been used for the treatment of gastrointestinal cancers [28]. In addition, a mTOR inhibitor is currently under investigation as a potential targeted therapy for malignancies [29]. Everolimus, an mTOR inhibitor, is effective against advanced, low, or intermediate grade PNETs [23]. mTOR is an evolutionarily conserved checkpoint protein kinase. mTOR, which acts downstream from the PI3K/Akt signaling pathway, is often upregulated in several cancer cells, and regulates cell growth, proliferation, motility, and survival. In addition, mTOR regulates protein synthesis by phosphorylating and activating of S6K and by phosphorylating and inactivating the mRNA translational repressor protein, 4E-BP1. S6K is a mitogen-activated serine/threonine protein kinase and required for cell growth and G1 cell cycle progression [30, 31]. S6K phosphorylates the S6 protein of the 40S ribosomal subunit, and participates in translating the 5′ oligopyrimidine tract mRNAs [30]. Despite being an indirect measurement of mTOR activity and lacking a clear function, S6K phosphorylation is widely used in both research and clinical practice as a biomarker of mTOR activity [6]. 4E-BP1, which also is a serine/threonine protein kinase, inhibits cap-dependent translation by binding to eIF4E. Phosphorylation of 4E-BP1 disrupts this interaction and subsequently activates cap-dependent translation [32].

Our findings demonstrate that the expression of mTOR, p-mTOR, S6K, and p-S6rp was associated with critical clinicopathological characteristics. For example, their expression was significantly related to vascular invasion, lymph node and/or distant metastasis, WHO classification, and ENETS TNM stage. In particular, lymph node and/or distant metastasis were an independent risk factor for a disease-free survival in this study, which correlated well with expression of p-mTOR, S6K, and p-S6rp. Furthermore, p-mTOR and p-S6rp expression was evident in areas near mitotic cells. In addition, a significant positive correlation was recognized between p-mTOR and p-S6rp. In contrast, the expression of 4E-BP1 and p-4E-BP1 was unrelated to the clinicopathological characteristics and not associated with the expression of p-mTOR. In a recent study on the pulmonary NETs, Righi et al. reported that levels of p-mTOR and expression of p-S6K were associated with more favorable clinicopathological characteristics but the expression of p-4E-BP1 was not [33]. Furthermore, it was reported that phosphorylation of some 4E-BP1 sites is relatively insensitive to rapamycin [8, 32]. In contrast, S6K regulation is sensitive to rapamycin, which indicates that the outputs from mTOR to 4E-BP1 and S6K are considerably distinct [8]. Therefore, S6K is a potential target of treatment for PNETs.

In recent studies, researchers have begun to focus on S6K inhibitors [34, 35]. Phase I clinical studies of LY2584702 (Eli Lilly and Co., Indianapolis, IN, USA), a selective S6K inhibitor, examined this drug for treatment of advanced solid tumors, as either a monotherapy [34] or combined therapy using erlotinib or everolimus [35]. They observed no partial or complete responses, and conducting further trials have been halted. However, Kasajima et al. demonstrated that the expression of activated S6K was related to a poor prognosis in 39 patients with stage 4 midgut NETs [27]. In addition, our study demonstrates clinical significance of S6K activation, and we believe the S6K inhibitor has potential for PNETs treatment. Further clinical trials performed with larger sample size are necessary to clarify these issues.

In conclusion, our finding suggests that the mTOR signaling pathway plays significant roles in tumorigenesis and progression of PNETs. In particular, activation of the S6K pathway may have clinical significance for both clinicians and researchers.

Acknowledgments We thank Ms Mayumi Takeda for her technical assistance. We also appreciate Dr Toshifumi Matsumoto (Beppu Medical Center), Dr Koichiro Tahara (Oita Medical Center) and Dr Seiichiro Kai (Oita Red Cross Hospital) for providing PNET samples.

Conflict of interest None declared.

References

1. Ong SL, Garcea G, Pollard CA, Furness PN, Steward WP, Rajesh A, et al. A fuller understanding of pancreatic neuroendocrine

tumours combined with aggressive management improves outcome. Pancreatology. 2009;5:583–600.
2. Khan A. Surgical pathology of endocrine and neuroendocrine tumors. New York: Springer; 2009.
3. Halfdanarson TR, Rabe KG, Rubin J, Petersen GM. Pancreatic neuroendocrine tumors (PNETs): incidence, prognosis and recent trend toward improved survival. Ann Oncol. 2008;10:1727–33.
4. Yao JC, Hassan M, Phan A, Dagohoy C, Leary C, Mares JE, et al. One hundred years after "carcinoid": epidemiology of and prognostic factors for neuroendocrine tumors in 35,825 cases in the United States. J Clin Oncol. 2008;26:3063–72.
5. Ito T, Sasano H, Tanaka M, Osamura RY, Kimura W, Takano K, et al. Epidemiological study of gastroenteropancreatic neuroendocrine tumors in Japan. J Gastroenterol. 2010;45:234–43.
6. Guertin DA, Sabatini DM. Defining the role of mTOR in cancer. Cancer Cell. 2007;12:9–22.
7. Fujiyoshi M, Ozaki M. Molecular mechanisms of liver regeneration and protection for treatment of liver dysfunction and diseases. J Hepatobiliary Pancreat Sci. 2011;18:13–22.
8. Wang X, Beugnet A, Murakami M, Yamanaka S, Proud CG. Distinct signaling events downstream of mTOR cooperate to mediate the effects of amino acids and insulin on initiation factor 4E-binding proteins. Mol Cell Biol. 2005;7:2558–72.
9. Wang X, Proud CG. The mTOR pathway in the control of protein synthesis. Physiology. 2006;21:362–9.
10. Hay N, Sonenberg N. Upstream and downstream of mTOR. Genes Dev. 2004;18:1926–45.
11. Altomare DA, Wang HQ, Skele KL, De Rienzo A, Klein-Szanto AJ, Godwin AK, et al. AKT and mTOR phosphorylation is frequently detected in ovarian cancer and can be targeted to disrupt ovarian tumor cell growth. Oncogene. 2004;23:5853–7.
12. No JH, Jeon YT, Park IA, Kim YB, Kim JW, Park NH, et al. Activation of mTOR signaling pathway associated with adverse prognostic factors of epithelial ovarian cancer. Gynecol Oncol. 2011;121:8–12.
13. Walsh S, Flanagan L, Quinn C, Evoy D, McDermott EW, Pierce A, et al. mTOR in breast cancer: differential expression in triple-negative and non-triple-negative tumors. Breast. 2012;21:178–82.
14. Sun CH, Chang YH, Pan CC. Activation of the PI3K/Akt/mTOR pathway correlates with tumour progression and reduced survival in patients with urothelial carcinoma of the urinary bladder. Histopathology. 2011;58:1054–63.
15. Herberger B, Puhalla H, Lehnert M, Wrba F, Novak S, Brandstetter A, et al. Activated mammalian target of rapamycin is an adverse prognostic factor in patients with biliary tract adenocarcinoma. Clin Cancer Res. 2007;13:4795–9.
16. Sahin F, Kannangai R, Adegbola O, Wang J, Su G, Torbenson M, et al. mTOR and p70S6 kinase expression in primary liver neoplasm. Clin Cancer Res. 2004;10:8421–5.
17. Li W, Tan D, Zhang Z, Liang JJ, Brown RE. Activation of Akt-mTOR-p70S6K pathway in angiogenesis in hepatocellular carcinoma. Oncol Rep. 2008;20:713–19.
18. Villanueva A, Chiang DY, Newell P, Peix J, Thung S, Alsinet C, et al. Pivotal role of mTOR signaling in hepatocellular carcinoma. Gastroenterology. 2008;135:1972–83.
19. Ballou LM, Lin RZ. Rapamycin and mTOR kinase inhibitors. J Chem Biol. 2008;1:27–36.
20. Mita MM, Mita AC, Chu QS, Rowinsky EK, Fetterly GJ, Goldston M, et al. Phase I trial of the novel mammalian target of rapamycin inhibitor deforolimus (AP23573; MK-8669) administered intravenously daily for 5 days every 2 weeks to patients with advanced malignancies. J Clin Oncol. 2008;26:361–7.
21. Rivera VM, Squillace RM, Miller D, Berk L, Wardwell SD, Ning Y, et al. Ridaforolimus (AP23573; MK-8669), a potent mTOR inhibitor, has broad antitumor activity and can be optimally administered using intermittent dosing regimens. Mol Cancer Ther. 2011;10:1059–71.
22. Yao JC, Shah MH, Ito T, Bohas CL, Wolin EM, Van Cutsem E, et al. Everolimus for advanced pancreatic neuroendocrine tumors. N Engl J Med. 2011;364:514–23.
23. Zhou CF, Ji J, Yuan F, Shi M, Zhang J, Liu BY, et al. mTOR activation in well differentiated pancreatic neuroendocrine tumors: a retrospective study on 34 cases. Hepatogastroenterology. 2011;58:2140–3.
24. Klimstra DS, Modlin IR, Coppola D, Lloyd RV, Suster S. The pathologic classification of neuroendocrine tumors: a review of nomenclature, grading, and staging systems. Pancreas. 2010;39:707–12.
25. Klöppel G, Rindi G, Perren A, Komminoth P, Klimstra DS. The ENETS and AJCC/UICC TNM classifications of the neuroendocrine tumors of the gastrointestinal tract and the pancreas: a statement. Virchows Arch. 2010;456:595–7.
26. Darb-Esfahani S, Faggad A, Noske A, Weichert W, Buckendahl AC, Müller B, et al. Phospho-mTOR and phospho-4EBP1 in endometrial adenocarcinoma: association with stage and grade in vivo and link with response to rapamycin treatment in vitro. J Cancer Res Clin Oncol. 2009;135:933–41.
27. Kasajima A, Pavel M, Derb-Esfahani S, Noske A, Sasano H, Dietel M, et al. mTOR expression and activity patterns in gastroenteropancreatic neuroendocrine tumors. Endocr Relat Cancer. 2011;18:181–92.
28. Durán I, Salazar R, Casanovas O, Arrazubi V, Vilar E, Siu LL, et al. New drug development in digestive neuroendocrine tumors. Ann Oncol. 2007;18:1307–13.
29. Pullen N, Thomas G. The modular phosphorylation and activation of p70S6K. FEBS Lett. 1997;410:78–82.
30. Dufuner A, Thomas G. Ribosomal S6 kinase signaling and the control of translation. Exp Cell Res. 1999;253:100–9.
31. Pause A, Belsham GJ, Gingras AC, Donzé O, Lin TA, Lawrence JC Jr, et al. Insulin-dependent stimulation of protein synthesis by phosphorylation of a regulator of 5′-cap function. Nature. 1994;371:762–7.
32. Gingras AC, Gygi SP, Raught B, Polakiewicz RD, Abraham RT, Hoekstra MF, et al. Regulation of 4E-BP1 phosphorylation: a novel two-step mechanism. Genes Dev. 1999;13:1422–37.
33. Righi L, Volante M, Rapa I, Tavaglione V, Inzani F, Pelosi G, et al. Mammalian target of rapamycin signaling activation patterns in neuroendocrine tumors of the lung. Endocr Relat Cancer. 2010;17:977–87.
34. Brail LH, Tolcher A, Goldman J, Patnaik A, Laux I, Papadopoulos K, et al. A phase 1 dose-escalation, pharmacokinetic (PK) and pharmacodynamic (PD) evaluation of oral LY2584702 a p70S6 kinase inhibitor. Ann Oncol. 2012;23(Suppl 1):i16.
35. Hollebecque A, Houede N, Cohen EEW, Italiano A, Yuan Z, Westwood P, et al. A phase 1 study of LY2584702, a p70S6 kinase inhibitor, with erlotinib or everolimus in patient with advanced solid tumors. Ann Oncol. 2012;23(Suppl 1):i16.

Surg Endosc (2014) 28:2466–2473
DOI 10.1007/s00464-014-3498-6

Effects of different pressure levels of CO_2 pneumoperitoneum on liver regeneration after liver resection in a rat model

Yoko Komori · Yukio Iwashita · Masayuki Ohta · Yuichiro Kawano · Masafumi Inomata · Seigo Kitano

Received: 30 October 2013 / Accepted: 17 February 2014 / Published online: 12 March 2014

Abstract
Background A recent study demonstrated that high pressure of carbon dioxide (CO_2) pneumoperitoneum before liver resection impairs postoperative liver regeneration. This study was aimed to investigate effects of varying insufflation pressures of CO_2 pneumoperitoneum on liver regeneration using a rat model.
Methods 180 male Wistar rats were randomly divided into three groups: control group (without preoperative pneumoperitoneum), low-pressure group (with preoperative pneumoperitoneum at 5 mmHg), and high-pressure group (with preoperative pneumoperitoneum at 10 mmHg). After pneumoperitoneum, all rats were subjected to 70 % partial hepatic resection and then euthanized at 0 min, 12 h, and on postoperative days (PODs) 1, 2, 4, and 7. Following outcome parameters were used: liver regeneration (liver regeneration rate, mitotic count, Ki-67 labeling index), hepatocellular damage (serum aminotransferases), oxidative stress [serum malondialdehyde (MDA)], interleukin-6 (IL-6), and hepatocyte growth factor (HGF) expression in the liver tissue.
Results No significant differences were observed for all parameters between control and low-pressure groups. The liver regeneration rate and mitotic count were significantly decreased in the high-pressure group than in control and low-pressure groups on PODs 2 and 4. Postoperative hepatocellular damage was significantly greater in the high-pressure group on PODs 1, 2, 4, and 7 compared with control and/or low-pressure groups. Serum MDA levels were significantly higher in the high-pressure group on PODs 1 and 2, and serum IL-6 levels were significantly higher in the high-pressure group at 12 h and on POD 1, compared with control and/or low-pressure groups. The HGF tissue expression was significantly lower in the high-pressure group at 12 h and on PODs 1 and 4, compared with that in control and/or low-pressure groups.
Conclusions High-pressure pneumoperitoneum before 70 % liver resection impairs postoperative liver regeneration, but low-pressure pneumoperitoneum has no adverse effects. This study suggests that following laparoscopic liver resection using appropriate pneumoperitoneum pressure, no impairment of liver regeneration occurs.

Keywords Liver regeneration · Laparoscopic liver resection · Pneumoperitoneum

Since introduction of laparoscopic cholecystectomy in 1987 [1], a laparoscopic approach has been applied to the full spectra of abdominal procedures. Since the first laparoscopic liver wedge resection was reported in 1992 [2], laparoscopic hepatectomy has been increasingly used in the field of hepatic surgery, and its use has exponentially increased worldwide in recent years [3, 4]. Current evidence from large series and reviews indicates that laparoscopic hepatectomy conveys benefits of minimally invasive surgery such as less analgesia requirement, shorter hospital stay, decreasing blood loss, delivering less operative morbidity, and better cosmesis [3, 5–8]. Furthermore, with improved development of laparoscopic instruments (such as dissection and coagulation devices), implementation of

Y. Komori (✉) · Y. Iwashita · M. Ohta · Y. Kawano · M. Inomata
Department of Gastroenterological and Pediatric Surgery, Oita University Faculty of Medicine, 1-1 Idaigaoka, Hasama-machi, Yufu, Oita 879-5593, Japan
e-mail: komorin@oita-u.ac.jp

S. Kitano
Oita University, Oita, Japan

hand-assisted techniques, and improvement of surgeons' laparoscopic skills, the trend in laparoscopic liver resection has now moved from limited resections toward performing major hepatectomies [9, 10].

However, it has been reported that laparoscopic surgeries can have numerous adverse effects, including oxidative stress in lung tissues [11], ischemia of various splanchnic organs [12], oxygen-free radical production [13], bacterial translocation [14], and carbon dioxide (CO_2) embolism [15]. A recent study of laparoscopic liver resection revealed that high intra-abdominal pressure decreases the amount of bleeding but increases the risk of CO_2 embolism [16]. Furthermore, experimental studies have demonstrated a reciprocal correlation between an increase in intra-abdominal pressure and portal vein flow reduction [17–20].

Moreover, a recent study using a rat model revealed that when rats were subjected to a 70 % hepatectomy, along with preoperative pneumoperitoneum of 9 mmHg for 60 min, the extended liver resection impaired postoperative liver regeneration [21]. However, another study demonstrated that pneumoperitoneal pressures of ≥8 mmHg in rats do not correspond to the routine working pressure employed in humans [22]. To create pneumoperitoneum in humans, laparoscopic surgeries involve insufflation of CO_2 into the peritoneal cavity at a rate of 4–6 l min^{-1} to a pressure of 10–15 mmHg [23]. Avital et al. [22] reported that pressures of ≥8 mmHg in rats correspond to pressures of ≥14–20 mmHg in humans, and a pressure of 5 mmHg is optimal in a rat model for simulating laparoscopy in humans. Therefore, we consider that the relationship between CO_2 pneumoperitoneum before liver resection and liver regeneration is not completely understood, and we designed our study to investigate how different pressure levels of CO_2 pneumoperitoneum affect liver regeneration following major hepatectomy.

Methods

Animals

In this study, all animal experiments used a total of 180 male Wistar rats weighing between 200 and 250 g (Kyudo Co., Ltd., Saga, Japan). All rats were provided unlimited access to food and water before and after treatment. All surgeries were performed under 3 % sevoflurane (Maruishi Pharmaceutical Co., Ltd., Osaka, Japan) anesthesia. This study was approved by the Animal Studies Committee of Oita University, Japan, and was performed according to the National Institutes of Health Standards of Animal Care.

Animal experiment protocol

Animals were divided into three groups of 60 rats each: 60 to undergo 60 min of anesthesia without CO_2 pneumoperitoneum followed by 70 % hepatectomy (control group), 60 to undergo 60 min of 5 mmHg pressure CO_2 pneumoperitoneum, followed by 70 % hepatectomy (low-pressure group), and 60 to undergo 60 min of 10 mmHg pressure CO_2 pneumoperitoneum, followed by 70 % hepatectomy (high-pressure group). The pneumoperitoneum was created using electronic insufflator (Surgiflator 9100, UHI-3, Olympus, Tokyo, Japan) through a 22-gauge extra tube (Surflo® I.V. catheter, Terumo®, Japan) and maintained with a continuous intra-abdominal pressure of 5 or 10 mmHg, as previously described [24].

After the pneumoperitoneum was created, the abdomen was desufflated through a median laparotomy for liver resection, and a 70 % partial hepatectomy was performed as previously described [25]. Middle and left lateral hepatic lobes were removed, and these lobes were ligated and resected using scissors. The total procedural time, including creating the pneumoperitoneum, was approximately 70 min for each group. After surgery, all rats received 5 ml of sterile isotonic saline subcutaneously to prevent dehydration. To analyze blood and liver tissue samples, 10 animals were euthanized at 0 min and 12 h after surgery and on postoperative days (PODs) 1, 2, 4, and 7, respectively, in each group. Blood samples were obtained using cardiac puncture aspiration. The liver was excised and weighed, and tissue samples were frozen in −80 °C or fixed in formaldehyde.

Liver regeneration rate

The liver regeneration rate was calculated as previously described [21, 26]. Briefly, the estimated whole liver weight was calculated, and the excised liver weight was calculated at 70 % of the whole liver weight. Therefore, the liver regeneration rate was calculated as follows: liver regeneration rate (%) $= 100 \times [C - (A - B)]/A$, where A represents the estimated whole liver weight, B represents the weight of the excised liver, and C represents the weight of the remnant liver at the time when the animal was euthanized.

Mitotic count and Ki-67 labeling index

Paraffin-embedded liver tissue samples were cut into 4-μm sections and stained with hematoxylin–eosin stain. The number of mitoses was counted using 10 high-power fields that were randomly selected under a light microscope.

In addition, deparaffinized hepatic sections (3-μm thick) were immunostained for Ki-67 using a mouse anti-rat Ki-67 antibody (MIB-5; Dako, Glostrup, Denmark). Positive hepatocytes were counted in 20 randomly selected high-power fields. In addition, the Ki-67 index was calculated per 1,000 hepatocytes.

Blood analyses of serum aminotransferases, malondialdehyde, and interleukin-6

Blood samples were immediately centrifuged. Serum aspartate aminotransferase (AST) and alanine aminotransferase (ALT) levels were determined using routine enzymatic methods as indicators of degrees of hepatocellular damage. Serum malondialdehyde (MDA) levels were measured as an indicator of oxidative stress, using a NWLSS kit from Northwest (Northwest Life Sciences Specialties, Vancouver, Canada), following the company protocol. Serum interleukin-6 (IL-6) levels were measured using commercially available rat enzyme-linked immunosorbent assay (ELISA) kits (Invitrogen, Inc., IL-6 Rat ELISA kit, Camarillo, CA).

Liver tissue expression of hepatocyte growth factor (HGF)

Tissue expression levels of HGF were measured from homogenized liver samples. Frozen liver tissue samples were homogenized using a tissue homogenizer (Dremel, Racine, WI, USA) and were subsequently centrifuged at 10,000×g for 10 min at 4 °C. HGF levels were measured using an assay kit following manufacturer's instructions (Institute of Immunology Co., Ltd., Rat HGF EIA, Tokyo, Japan). Absorbance at 586 nm was determined using an ELISA reader (Bio-Rad Laboratories).

Statistical analysis

All data are presented as mean ± standard deviation. All data were evaluated using one-way analysis of variance with the Bonferroni test for multiple comparisons. A value of $p < 0.05$ was considered to be statistically significant. Statistical analyses were performed using SPSS II (version 11.01 J; SPSS Japan, Inc., Tokyo, Japan).

Results

Effects of pneumoperitoneum pressures on liver regeneration

Results indicated that preoperative high-pressure pneumoperitoneum inhibited liver regeneration following hepatectomy. Gravimetric analysis revealed that liver regeneration rate was significantly lower in the high-pressure group on PODs 2 and 4 compared with that in control ($p = 0.003$, 0.004, respectively, Fig. 1) and low-pressure groups ($p = 0.000$, 0.005, respectively). The mitotic count was significantly lower in the high-pressure group on PODs 2 and 4 compared with that in control group ($p = 0.006$, 0.048, respectively) and on POD 2 than in the low-pressure group ($p = 0.0032$). Moreover, Ki-67 expression levels were significantly lower in the high-pressure group on PODs 1 and 2 compared with control ($p = 0.000$, 0.018, respectively) and low-pressure groups ($p = 0.0015$, 0.0016, respectively).

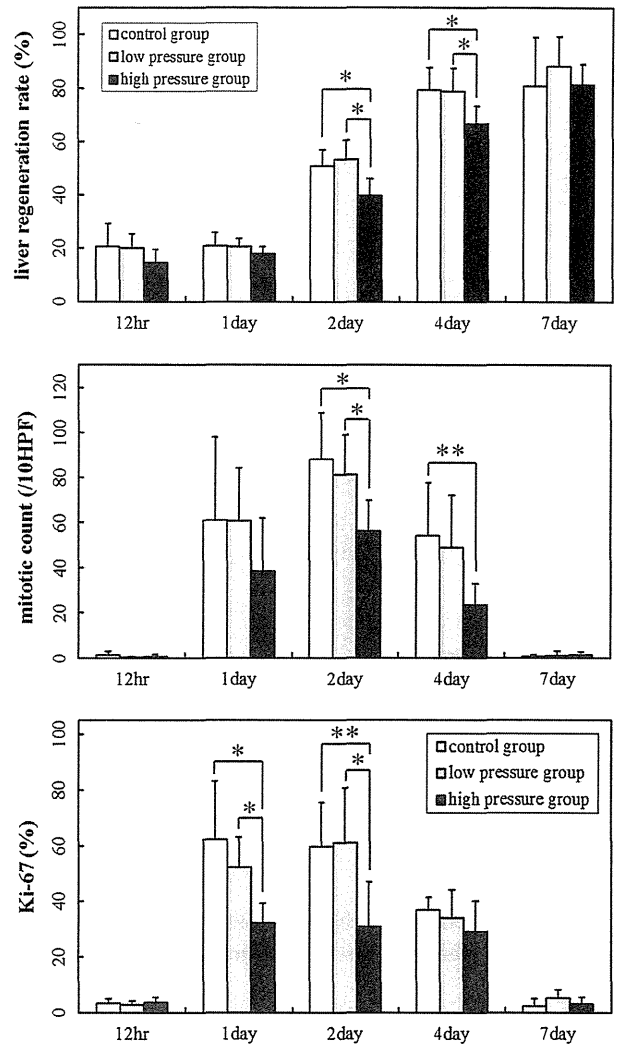

Fig. 1 Effects of carbon dioxide pneumoperitoneum following 70 % hepatectomy on liver regeneration in control, low-pressure, and high-pressure groups. Represented by the liver regeneration rate, mitotic count, and Ki-67 labeling index at different postoperative time points. Each point consists of 10 rats. *$p < 0.01$, **$p < 0.05$

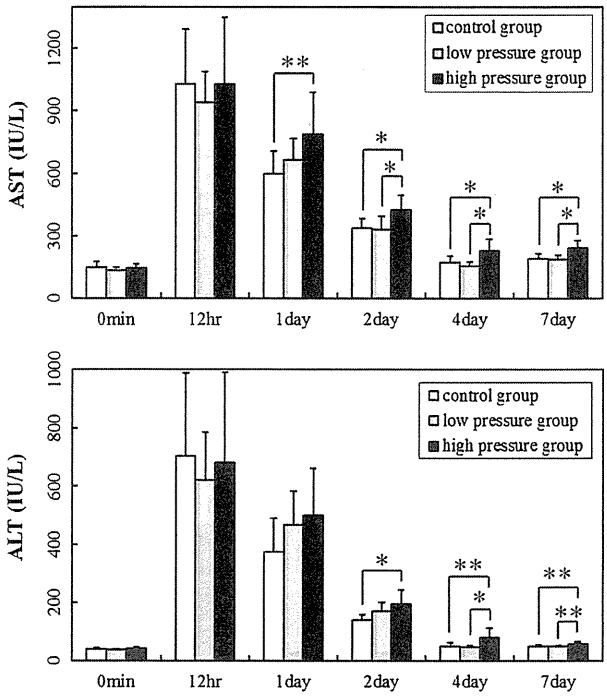

Fig. 2 Hepatocellular damage after 70 % hepatectomy in control, low-pressure, and high-pressure groups. Represented by serum levels of aspartate aminotransferase (AST) and alanine aminotransferase (ALT) at different postoperative time points. Each point consists of 10 rats. $*p < 0.01$, $**p < 0.05$

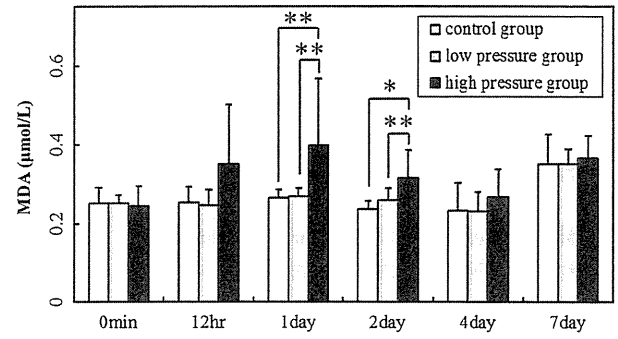

Fig. 3 Oxidative stress following 70 % hepatectomy in control, low-pressure, and high-pressure groups. Represented by serum malondialdehyde (MDA) levels at different postoperative time points. Each point consists of 10 rats. $*p < 0.01$, $**p < 0.05$

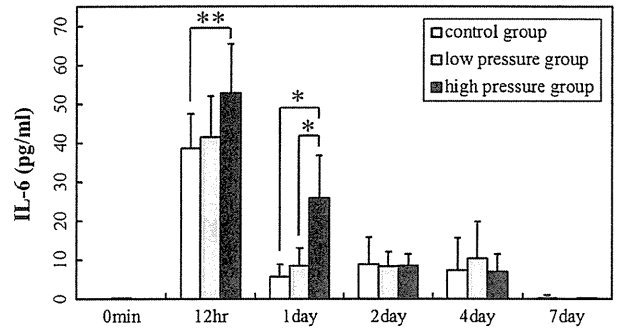

Fig. 4 Postoperative data of interleukin-6 (IL-6) following 70 % hepatectomy in control, low-pressure, and high-pressure groups at different postoperative time points. Each point consists of 10 rats. $*p < 0.01$, $**p < 0.05$

Effects of pneumoperitoneum pressures on liver damage, changes of oxidative stress, and cytokine levels

Greater liver damage was recognized in the high-pressure group. These animals revealed significantly higher AST levels on PODs 1, 2, 4, and 7 compared with those in control group ($p = 0.022$, 0.009, 0.009, 0.001, respectively, Fig. 2) and on PODs 2, 4, and 7 compared with those in the low-pressure group ($p = 0.003$, 0.001, 0.001, respectively). Animals in the high-pressure group revealed significantly higher ALT levels on PODs 2, 4, and 7 compared with those in control group ($p = 0.004$, 0.010, 0.041, respectively) and on PODs 4 and 7 compared with those in the low-pressure group ($p = 0.003$, 0.020, respectively).

The group with a high-pressure CO_2 pneumoperitoneum revealed a significantly increased oxidative stress reaction. These animals revealed significantly higher serum MDA levels on PODs 1 and 2 compared with those in control ($p = 0.019$, 0.002, respectively, Fig. 3) and low-pressure groups ($p = 0.021$, 0.031, respectively). Serum IL-6 levels were significantly higher in the high-pressure group at 12 h compared with those in the control group ($p = 0.028$, Fig. 4), and on POD 1 compared with those in control ($p = 0.000$) and low-pressure groups ($p = 0.000$).

Effects of pneumoperitoneum pressures on the tissue expression of HGF

Tissue expression levels of HGF were significantly lower in the high-pressure group at 12 h and on PODs 1 and 4 compared with those in the control group ($p = 0.049$, 0.028, 0.034, respectively, Fig. 5) and at 12 h and on POD 4 compared with those in the low-pressure group ($p = 0.044$, 0.006, respectively).

Discussion

Laparoscopic hepatectomy is being increasingly used in the field of hepatic surgery. Recent studies demonstrate that minimally invasive hepatic resection for benign and malignant tumors is safe and feasible with definite short-

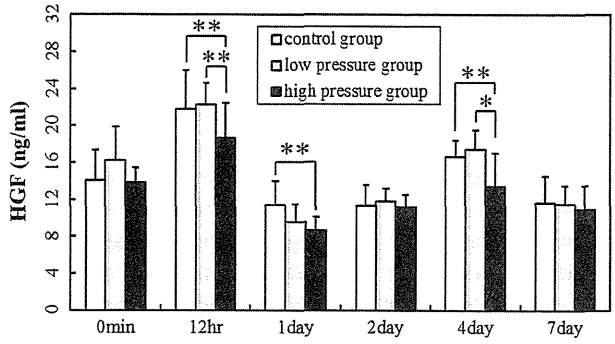

Fig. 5 Tissue expression of hepatocyte growth factor (HGF) following 70 % hepatectomy in control, low-pressure, and high-pressure groups at different postoperative time points. Each point consists of 10 rats. $*p < 0.01$, $**p < 0.05$

term benefits, no economic disadvantage, and no compromise of oncological principles [3, 7, 27]. Literature contains reports of 2,804 laparoscopic hepatic resections for both benign and malignant tumors with a perioperative mortality of 0.3 % and morbidity of 10.5 % [5].

However, apart from technical and oncological considerations, there have been several reports related to potential adverse effects of CO_2 pneumoperitoneum on liver function following laparoscopic surgery [27–30]. Clinical and experimental studies have reported that increased intra-abdominal pressure generated by pneumoperitoneum causes a marked decrease in cardiovascular hemodynamics and splanchnic and portal blood flow [12, 17–20, 30, 31]. Splanchnic ischemia may result in the conversion of oxygen into free radicals in tissues undergoing reperfusion [32, 33]. Some authors suggest that adverse effects of pneumoperitoneum are possibly a result of an ischemia–reperfusion phenomenon induced by the inflation and deflation of the pneumoperitoneum [13, 14, 29]. Laparoscopic cholecystectomy with 14 mmHg CO_2 pneumoperitoneum significantly increased AST and ALT levels [28]. In another clinical study, laparoscopic cholecystectomy with 14 mmHg pneumoperitoneum significantly increased cytolytic enzyme levels compared with those with 10 mmHg pneumoperitoneum [30, 31]. Furthermore, it is well known that ischemia–reperfusion injury of the liver impairs liver regeneration after partial hepatectomy in experiments with animals [34–36].

Regarding another mechanism of liver injury under CO_2 pneumoperitoneum, blood levels of pH, CO_2, and HCO_3 might be related to the injury. Hazebroek et al. [37] investigated effects of pneumoperitoneum at 6 or 12 mmHg on arterial pH, PCO_2 and HCO_3 in a rat model. CO_2 insufflation caused a significant decrease in arterial pH at both 6 and 12 mmHg, a significant increase in $PaCO_2$ at 6 mmHg pressure, and a significant decrease in arterial HCO_3 at 12 mmHg. However, recently, Nickkholgh et al. [38] performed the similar study. While arterial pH was significantly decreased under CO_2 pneumoperitoneum at 8 and 12 mmHg pressures, arterial levels of CO_2 and HCO_3 were not significantly changed compared with the control without pneumoperitoneum. Therefore, the authors concluded that the cause of liver damage induced by CO_2 pneumoperitoneum was ischemia–reperfusion injury.

Some literature has reported that pneumoperitoneum in association with partial hepatectomy or extended hepatectomy leads to a reduction in postoperative liver regeneration [21, 39, 40]. Kaya et al. [39] observed a significant reduction in liver regeneration on PODs 1 and 4 after partial hepatectomy followed by pneumoperitoneum of 12–14 mmHg for 24 h. In addition, Yagmurdur et al. [40] revealed an impairment of liver regeneration on POD 5 in rats subjected to a 15 mmHg pneumoperitoneum for 60 min followed by partial hepatectomy. In a most recent research, Schmidt et al. [21] subjected rats to a 70 % hepatectomy with preoperative pneumoperitoneum of 9 mmHg for 60 min and demonstrated that pneumoperitoneum before extended liver resection impaired postoperative liver regeneration.

However, Avital et al. [22] demonstrated that a pressure of ≥8 mmHg in a rat model corresponds to a human pressure of ≥14–20 mmHg, causing maximal ventilator pressure and supraphysiologic $ETCO_2$ they concluded that a pressure of 5 mmHg is optimal in a rat model to simulate laparoscopy in humans. Further, Gagner [41] cited this paper, emphasizing that the pressure chosen for pneumoperitoneum in rats is important and that pressures of ≥8 mmHg do not correspond to pressures used in humans because of the much smaller abdominal cavity and lesser compliance of the abdominal wall, thereby causing hemodynamic effects that are only seen in humans when pressures are used at supraphysiological levels. Therefore, in our experimental setting, we used a low-pressure pneumoperitoneum of 5 mmHg (low-pressure group) and high-pressure pneumoperitoneum of 10 mmHg (high-pressure group) and investigated liver damage and regeneration at different time points.

In the present study, we received logical results in serum liver enzymes, oxidative stress, cytokine, and liver regeneration. A comparison of three groups (control, low-pressure, and high-pressure groups) revealed that any significantly different results for parameters appeared only in the high-pressure group when it was compared to the control group. For the liver regeneration rate, a positive impact was observed in control and low-pressure groups compared with the high-pressure group on PODs 2 and 4. In addition, we found a marked proliferative activity (evident from an increased mitotic count) in control and low-pressure groups on PODs 2 and 4 compared with the high-pressure group. Similarly, the Ki-67 labeling index

was significantly higher in control and low-pressure groups on PODs 1 and 2 compared with that in the high-pressure group. Corresponding to the outcome of liver regeneration and mitotic activity, tissue expression levels of HGF were significantly higher in control and low-pressure groups at 12 h and on PODs 1 and 4, respectively, compared with those in the high-pressure group. These results suggest that appropriate pressure levels of pneumoperitoneum do not influence liver regeneration following major hepatectomy, and to our knowledge, this is probably the first report on different effects from varying CO_2 pressure levels on liver regeneration.

CO_2 pneumoperitoneum causes a reduction in splanchnic blood flow, resulting in biochemical evidence of oxidative stress in a pressure- and time-dependent manner [42]. MDA is the end product of lipid peroxidation, and MDA levels in liver homogenate or serum are a direct marker of levels of oxygen radicals [43]. In this study, we found that serum MDA levels were significantly increased in the high-pressure group on PODs 1 and 2 compared with those in control and low-pressure groups, indicating that oxygen radicals are increased after exposure to high-pressure pneumoperitoneum. In addition, it is well known that organ ischemia activates inflammatory cytokines. IL-6 is an integral cytokine mediator of the acute phase of response to injury and infection [44]. IL-6 is often induced along with inflammatory cytokines TNFα and IL-1 in several critical conditions, and circulating IL-6 plays an important role in the induction of acute phase reactions [45]. The IL-6 response to injury is consistent and is related to the magnitude of the insult [44]. In this study, higher levels of serum IL-6 in the high-pressure group at 12 h and on POD 1 were recognized, and these data demonstrate that the high-pressure group received greater injury to the liver compared with other groups.

At several high-volume centers, laparoscopic hepatectomy is clinically performed at a CO_2 pneumoperitoneal pressure of <12 mmHg [46]. However, several clinical studies on laparoscopic hepatectomy suggest that a high-pneumoperitoneal pressure is effective in controlling bleeding during liver parenchymal transection [47, 48]. In fact, Cannon et al. [49] used pressures of 12–15 mmHg to control the bleeding from veins on the surface of the transected liver. In this study, no significant differences were observed in control and low-pressure groups, and the high-pressure group only revealed adverse effects in liver regeneration with significant differences. Most previous studies revealing the adverse effects of CO_2 pneumoperitoneum have used pneumoperitoneal pressures of ≥14 mmHg in human studies and ≥8 mmHg in rat models [13, 14, 21, 28, 39, 43]. We believe that the different effects noted between low- and high-pressure pneumoperitoneum could be related to the alteration of hepatic blood flow and ischemia–reperfusion injury, causing production of oxygen-derived free radicals and inflammatory cytokines that contributed to organ dysfunction. Some researchers have demonstrated that the creation of a CO_2 pneumoperitoneum with an increase in intra-abdominal pressure leads to a linear decrease in portal venous flow in rats [17, 18, 20]. Leister et al. [50] investigated differences between a 4 and 8 mmHg pneumoperitoneum on hepatobiliary excretion (as a sensitive indicator of liver function) in a rat model; although no significant alteration was observed in the bile flow under the 4 mmHg pneumoperitoneum, biliary excretion was considerably reduced under the 8-mmHg pneumoperitoneum.

To prevent liver injury under CO_2 pneumoperitoneum, it has been thought to be beneficial to use another gas and/or perform ischemic preconditioning. Some animal studies have compared CO_2 gas insufflation with helium gas insufflation. The helium gas is superior to CO_2 gas in the terms of changes in arterial levels of pH, CO_2, and HCO_3, and in portal blood flow [18, 37]. However, helium has some disadvantages. Helium is not only expensive compared with CO_2 but also has lower solubility in blood than CO_2 [51]. Some animal studies also demonstrated that the ischemic preconditioning conducted by short time CO_2 deflation after short time CO_2 insufflation can prevent ischemia–reperfusion injury afterward [52–54]. Therefore, the further clinical study of ischemic preconditioning is thought to be necessary.

In conclusion, this study demonstrates that pressure levels of the pneumoperitoneum are related to postoperative alteration in liver regeneration following hepatectomy. An appropriate pressure does not impair liver regeneration following laparoscopic liver resection. However, further experimental and clinical trials are necessary to ascertain an appropriate pneumoperitoneal pressure when performing laparoscopic hepatectomy.

Acknowledgments We are grateful to Ms. Mayumi Takeda for her technical assistance.

Disclosures The authors declare no conflicts of interest. No financial support was received for this study.

References

1. Polychronidis A, Laftsidis P, Bounovas A, Simopoulos C (2008) Twenty years of laparoscopic cholecystectomy: Philippe Mouret—March 17, 1987. JSLS 12(1):109–111
2. Gagner M, Rheault M, Dubuc J (1992) Laparoscopic partial hepatectomy for liver tumor. Surg Endosc 6:97–98
3. Lee KF, Chong CN, Wong J, Cheung YS, Wong J, Lai P (2011) Long-term results of laparoscopic hepatectomy versus open hepatectomy for hepatocellular carcinoma: a case-matched analysis. World J Surg 35(10):2268–2274

4. Abu HM, Di FF, Syed S, Wiltshire R, Dimovska E, Turner D, Primrose JN, Pearce NW (2013) Assessment of the financial implications for laparoscopic liver surgery: a single-centre UK cost analysis for minor and major hepatectomy. Surg Endosc 27(7):2542–2550
5. Nguyen KT, Gamblin TC, Geller DA (2009) World review of laparoscopic liver resection: 2,804 patients. Ann Surg 250(5): 831–841
6. Viganò L, Tayar C, Laurent A, Cherqui D (2009) Laparoscopic liver resection: a systematic review. J Hepatobiliary Pancreat Surg 16(4):410–421
7. Nguyen KT, Marsh JW, Tsung A, Steel JJ, Gamblin TC, Geller DA (2011) Comparative benefits of laparoscopic vs open hepatic resection: a critical appraisal. Arch Surg 146(3):348–356
8. Nitta H, Sasaki A, Fujita T, Itabashi H, Hoshikawa K, Takahara T, Takahashi M, Nishizuka S, Wakabayashi G (2010) Laparoscopy-assisted major liver resections employing a hanging technique: the original procedure. Ann Surg 251(3):450–453
9. Lin NC, Nitta H, Wakabayashi G (2013) Laparoscopic major hepatectomy: a systematic literature review and comparison of 3 techniques. Ann Surg 257:205–213
10. Dagher I, O'Rourke N, Geller DA, Cherqui D, Belli G, Gamblin TC, Lainas P, Laurent A, Nguyen KT, Marvin MR, Thomas M, Ravindra K, Fielding G, Franco D, Buell JF (2009) Laparoscopic major hepatectomy: an evolution in standard of care. Ann Surg 250(5):856–860
11. Pross M, Schulz HU, Flechsig A, Manger T, Halangk W, Augustin W, Lippert H, Reinheckel T (2000) Oxidative stress in lung tissue induced by CO_2 pneumoperitoneum in the rat. Surg Endosc 14(12):1180–1184
12. Schäfer M, Sägesser H, Reichen J, Krähenbühl L (2001) Alterations in hemodynamics and hepatic and splanchnic circulation during laparoscopy in rats. Surg Endosc 15:1197–1201
13. Eleftheriadis E, Kotzampassi K, Papanotas K, Heliadis N, Sarris K (1996) Gut ischemia, oxidative stress, and bacterial translocation in elevated abdominal pressure in rats. World J Surg 20: 11–16
14. Polat C, Aktepe OC, Akbulut G, Yilmaz S, Arikan Y, Dilek ON, Gokce O (2003) The effects of increased intra-abdominal pressure on bacterial translocation. Yonsei Med J 44(2):259–264
15. Smith HS (2011) Carbon dioxide embolism during pneumoperitoneum for laparoscopic surgery: a case report. AANA J 79: 371–373
16. Eiriksson K, Fors D, Rubertsson S, Arvidsson D (2011) High intra-abdominal pressure during experimental laparoscopic liver resection reduces bleeding but increases the risk of gas embolism. Br J Surg 98(6):845–852
17. Gutt CN, Schmandra TC (1999) Portal venous flow during CO_2 pneumoperitoneum in the rat. Surg Endosc 13:902–905
18. Schmandra TC, Kim ZG, Gutt CN (2001) Effect of insufflation gas and intraabdominal pressure on portal venous flow during pneumoperitoneum in the rat. Surg Endosc 15:405–408
19. Jakimowicz J, Stultiëns G, Smulders F (1998) Laparoscopic insufflation of the abdomen reduces portal venous flow. Surg Endosc 12(2):129–132
20. Richter S, Olinger A, Hildebrandt U, Menger MD, Vollmar B (2001) Loss of physiologic hepatic blood flow control ("hepatic arterial buffer response") during CO_2 pneumoperitoneum in the rat. Anesth Analg 93:872–877
21. Schmidt SC, Schumacher G, Klage N, Chopra S, Neuhaus P, Neumann U (2010) The impact of carbon dioxide pneumoperitoneum on liver regeneration after liver resection in a rat model. Surg Endosc 24:1–8
22. Avital S, Itash R, Szomstein S, Rosenthal R, Inbar R, Sckornik Y, Weinbroum A (2009) Correlation of CO_2 pneumoperitoneal pressures between rodents and humans. Surg Endosc 23(1):50–54
23. Perrin M, Fletcher A (2004) Laparoscopic abdominal surgery. Contin Educ Anaesth Crit Care Pain 4(4):107–110
24. Matsumoto T, Tsuboi S, Dolgor B, Bandoh T, Yoshida T, Kitano S (2001) The effect of gases in the intraperitoneal space on cytokine response and bacterial translocation in a rat model. Surg Endosc 15:80–84
25. Martins PNA, Theruvath TP, Neuhaus P (2007) Rodent models of partial hepatectomies. Liver Int 28:3–11
26. Okano T, Ohwada S, Nakasone Y, Sato Y, Ogawa T, Tago K, Morishita Y (2001) Blood transfusion causes deterioration in liver regeneration after partial hepatectomy in rats. J Surg Res 101(2):157–165
27. Endo Y, Ohta M, Sasaki A et al (2007) A comparative study of the long-term outcomes after laparoscopy-assisted and open left lateral hepatectomy for hepatocellular carcinoma. Surg Laparosc Endosc Percutan Tech 19:171–174
28. Güven HE, Oral S (2007) Liver enzyme alterations after laparoscopic cholecystectomy. J Gastrointest Liver Dis 16:391–394
29. Glantzounis GK, Tselepis AD, Tambaki AP, Trikalinos TA, Manataki AD, Galaris DA, Tsimoyiannis EC, Kappas AM (2001) Laparoscopic surgery-induced changes in oxidative stress markers in human plasma. Surg Endosc 15:1315–1319
30. Eryılmaz HB, Memis D, Sezer A, Inal MT (2012) The effects of different insufflation pressures on liver functions assessed with LiMON on patients undergoing laparoscopic cholecystectomy. Sci World J. doi:10.1100/2012/172575 (Epub 24 April 2012)
31. Morino M, Giraudo G, Festa V (1998) Alterations in hepatic function during laparoscopic surgery: an experimental clinical study. Surg Endosc 12:968–972
32. Ferrari R (1994) Oxygen-Free radicals at myocardial level: effects of ischemia and reperfusion. Adv Exp Med Biol 366: 99–111
33. Kloner RA, Przyklenk K, Whittaker P (1989) Deleterious effects of oxygen radicals in ischemia/reperfusion. Resolved and unresolved issues. Circulation 80:1115–1127
34. Foschi D, Castoldi L, Lesma A, Musazzi M, Benevento A, Trabucchi E (1993) Effects of ischaemia and reperfusion on liver regeneration in rats. Eur J Surg 59:393–398
35. Camargo CA Jr, Madden JF, Gao W, Selvan RS, Clavien PA (1997) Interleukin-6 protects liver against warm ischemia/reperfusion injury and promotes hepatocyte proliferation in the rodent. Hepatology 26(6):1513–1520
36. Usami M, Furuchi K, Shiroiwa H, Saitoh Y (1994) Effect of repeated portal-triad cross-clamping during partial hepatectomy on hepatic regeneration in normal and cirrhotic rats. J Surg Res 57(5):541–548
37. Hazebroek EJ, Haitsma JJ, Lachmann B, Steyerberg EW, de Bruin RW, Bouvy ND, Bonjer HJ (2002) Impact of carbon dioxide and helium insufflation on cardiorespiratory function during prolonged pneumoperitoneum in an experimental rat model. Surg Endosc 16:1073–1078
38. Nickkholgh A, Barro-Bejarano M, Liang R, Zorn M, Mehrabi A, Gebhard MM, Büchler MW, Gutt CN, Schemmer P (2008) Signs of reperfusion injury following CO_2 pneumoperitoneum: an in vivo microscopy study. Surg Endosc 22:122–128
39. Kaya Y, Aral W, Coskun T, Erkasap N, Var A (2002) Increased intraabdominal pressure impairs liver regeneration after partial hepatectomy in rats. J Surg Res 108:250–257
40. Yagmurdur MC, Basaran O, Ozdemir H, Gur G, Turan M, Karakayali H, Haberal M (2004) The impact of transient elevation of intraabdominal pressure on liver regeneration in the rat. J Investig Surg 17:315–322
41. Gagner M (2010) High-pressure carbon dioxide pneumoperitoneum before major liver resection in a rat model is not realistic and cannot be transposed to humans when studying liver regeneration. Surg Endosc 25:988–989

42. Sammour T, Mittal A, Loveday BP, Kahokehr A, Phillips AR, Windsor JA, Hill AG (2009) Systematic review of oxidative stress associated with pneumoperitoneum. Br J Surg 96:836–850
43. Xu GS, Liu HN, Li J, Wu XL, Dai XM, Liu YH (2009) Hepatic injury induced by carbon dioxide pneumoperitoneum in experimental rats. World J Gastroenterol 15(24):3060–3064
44. Biffl WL, Moore EE, Moore FA, Peterson VM (1996) Interleukin-6 in the injured patient marker of injury or mediator of inflammation? Ann Surg 224:647–664
45. Xing Z, Gauldie J, Cox G, Baumann H, Jordana M, Lei XF, Achong MK (1998) IL-6 is an antiinflammatory cytokine required for controlling local or systemic acute inflammatory responses. J Clin Investig 101:311–320
46. Otsuka Y, Katagiri T, Ishii J, Maeda T, Kubota Y, Tamura A, Tsuchiya M, Kaneko H (2013) Gas embolism in laparoscopic hepatectomy: what is the optimal pneumoperitoneal pressure for laparoscopic major hepatectomy? J Hepatobiliary Pancreat Sci 20:137–140
47. Are C, Fong Y, Geller DA (2005) Laparoscopic liver resection. Adv Surg 39:57–75
48. Buell JF, Koffron AJ, Thomas MJ, Rudich S, Abecassis M, Woodle ES (2005) Laparoscopic liver resection. J Am Coll Surg 200:472–480
49. Cannon RM, Brock GN, Marvin MR, Buell JF (2011) Laparoscopic liver resection: an examination of our first 300 patients. J Am Coll Surg 213:501–507
50. Leister I, Schüler P, Vollmar B, Füzesi L, Kahler E, Becker H, Markus PM (2004) Microcirculation and excretory function of the liver under conditions of carbon dioxide pneumoperitoneum. Surg Endosc 18:1358–1363
51. Junghans T, Böhm B, Meyer E (2000) Influence of nitrous oxide anesthesia on venous gas embolism with carbon dioxide and helium during pneumoperitoneum. Surg Endosc 14:1167–1170
52. Nesek-Adam V, Rasić Z, Vnuk D, Schwarz D, Rasić D, Crvenković D (2010) Ischemic preconditioning decreases laparoscopy induced oxidative stress in the liver. Coll Antropol 34:571–576
53. Cevrioglu AS, Yilmaz S, Koken T, Tokyol C, Yilmazer M, Fenkci IV (2004) Comparison of the effects of low intra-abdominal pressure and ischaemic preconditioning on the generation of oxidative stress markers and inflammatory cytokines during laparoscopy in rats. Hum Reprod 19:2144–2151
54. Avraamidou A, Marinis A, Asonitis S, Perrea D, Polymeneas G, Voros D, Argyra E (2012) The impact of ischemic preconditioning on hemodynamic, biochemical and inflammatory alterations induced by intra-abdominal hypertension: an experimental study in a porcine model. Langenbecks Arch Surg 397:1333–1341

Surg Today (2014) 44:1744–1750
DOI 10.1007/s00595-013-0749-4

ORIGINAL ARTICLE

Effects of the dihydrolipoyl histidinate zinc complex against carbon tetrachloride-induced hepatic fibrosis in rats

Yuichiro Kawano · Masayuki Ohta · Yukio Iwashita · Yoko Komori · Masafumi Inomata · Seigo Kitano

Received: 10 May 2013 / Accepted: 22 August 2013 / Published online: 12 October 2013

Abstract
Purpose This study investigated the effects of an antioxidant, dihydrolipoyl histidinate zinc complex (DHLHZn), on the hepatic fibrosis in the carbon tetrachloride (CCl_4) rat model.
Methods The animals were divided into three groups: control, CCl_4, and CCl_4+DHLHZn. A histological assessment of the liver fibrosis was performed using stained liver samples. The oxidative stress and antioxidant levels were evaluated by measuring the malondialdehyde (MDA) and glutathione (GSH) levels in the liver. In addition, cultured human hepatic stellate cells (LI90) were exposed to antimycin-A (AMA) and divided into four groups: control, DHLHZn, AMA, and AMA+DHLHZn. The effects of DHLHZn on AMA-induced fibrosis were evaluated by measuring the expression of transforming growth factor (TGF)-β1 and collagen α1 (I).
Results The hepatic fibrosis in the CCl_4+DHLHZn group was attenuated compared to that in the CCl_4 group. The MDA levels in the CCl_4+DHLHZn group were significantly lower than those of the CCl_4 group, whereas the GSH levels in the CCl_4+DHLHZn group were significantly higher than those of the CCl_4 group. Furthermore, the relative mRNA expression of TGF-β1 and collagen α1 (I) in the AMA+DHLHZn group was significantly lower than that in the AMA group.
Conclusion DHLHZn may attenuate the hepatic fibrosis induced by CCl_4 by decreasing the degree of oxidative stress.

Keywords Carbon tetrachloride (CCl_4) · Hepatic fibrosis · Oxidative stress · Antioxidant · Hepatic stellate cell

Introduction

Hepatic fibrosis is a pathological outcome induced by various chronic hepatic injuries [1]. The primary causes of liver fibrosis include viral hepatitis, alcohol use, autoimmune disorders, drugs and biliary obstruction [2]. An increase in reactive oxygen species (ROS) and free radicals may cause a break in the antioxidant defense of the liver, thereby contributing to the induction of fibrosis [3, 4]. Carbon tetrachloride (CCl_4) is widely used to generate hepatic fibrosis in model animals, as well as to induce rapid liver damage from steatosis and centrilobular necrosis [5, 6]. CCl_4 stimulates the formation of free radicals, ROS and lipid peroxidation products, which cause hepatic cell damage and necrosis [7–9]. Hepatic stellate cells (HSCs), which are mesenchymal cells in the space of Disse, produce the extracellular matrix that induces hepatic fibrosis [10, 11]. HSCs play an important role in the cellular events which lead to fibrosis [12]. During liver injury, these cells change to exhibit a myofibroblast-like phenotype and secrete extracellular matrix components [13]. The ROS levels are increased during the process of liver fibrosis [14, 15]; consequently, these increased levels stimulate HSC activation and collagen deposition [16].

Y. Kawano (✉) · M. Ohta · Y. Iwashita · Y. Komori · M. Inomata
Department of Gastroenterological and Pediatric Surgery, Faculty of Medicine, Oita University, 1-1 Idaigaoka, Hasama-machi, Yufu, Oita 879-5593, Japan
e-mail: yukawano@oita-u.ac.jp

S. Kitano
Oita University, 1-1 Idaigaoka, Hasama-machi, Yufu, Oita 879-5593, Japan